JOURNAL OF MATERIALS SCIENCE 24 (1989) 1479–1485

Low voltage electrical properties of polypropylene filled with stainless steel fibres and a model of sample conductivity based on fibre geometry

B. BRIDGE*, M. J. FOLKES‡, H. JAHANKHANI‡
*Departments of *Physics and ‡Materials Technology, Brunel University, Kingston Lane, Uxbridge, Middlesex, UB8 3PH, UK*

The d.c. electrical properties of 80 × 80 × 3 mm^3 polypropylene plaques filled with 6.5 μm diameter stainless steel fibres have been studied for volume fractions in the vicinity of a critical threshold at which the volume resistivity changes very rapidly with filler concentration. By the use of very low power inputs to eliminate any possibility of local temperature changes, the samples have been established to be ohmic conductors with resistivities ranging from 12 to 0.61 Ω cm for fibre volume fractions of 1 to 3%. It is suggested that percolation conditions i.e. continuous chains of metal fibres are produced at low volume fraction of filler because of a special fibre geometry i.e. a substantial proportion of the fibres are three dimensionally folded into shapes of roughly helical form, thus enhancing the probabilities of contact between adjacent fibres. For simplicity a model structure of perfect helices with identical diameters and pitch has been examined. The model leads to a critical volume fraction at the percolation threshold, which is in good agreement with experiment and proportional to the square of the ratio of fibre diameter to helix diameter. The threshold resistivity range predicted by the model is also a function of fibre and helix diameter and this resistivity also decreases with mean fibre length. It is argued further that there exists an optimum value of fibre aspect ratio for which the critical volume fraction is a minimum. The predicted threshold resistivity is in good agreement with experiment providing that a small amount of the size coating is assumed to have been removed during manufacture of the plaques, thus allowing a small fraction of the fibre–fibre contacts to be conducting.

1. Introduction

In recent years [1–6] polymers have become widely employed for the construction of electronic equipment enclosures and cabinetry. Polymers are attractive because they are cost-effective and avoid the labour intensive processing and finishing steps that metal components require. They have the advantage of being readily mouldable into convenient shapes. To shield against electromagnetic interference (EMI) effectively, a plastic equipment enclosure or cabinet must be made electrically conductive either with a secondary conductive coating such as zinc, nickel, or silver, or by addition of a conductive filler to the plastic compound. So far each of the available shielding methods has certain inherent disadvantages. Secondary coatings require an extra production step, while conductive fillers alter the characteristics of the resin in the composite. The authors are working on the optimization of the design of conducting polymers composites having stainless steel fibres as the conduction-enhancing filler. Metal fibre fillers have advantages over other fillers such as colloidal metals, fibrous or particulate carbon, in that modification of the microstructure of the matrix may be minimized and the mechanical performance optimized. Compared with other metals, stainless steel fibres combine the useful attributes of being relatively inexpensive, non-magnetic thus aiding dispersal, and resistant against breakage during processing. With regard to the latter property, it is now well established [7, 8] that the levels of bulk conductivity that can be achieved with a given filler volume fraction increases with fibre aspect ratio.

A frequent complaint heard amongst those involved in research and development work on particulate or fibre filled conductive composites, is that of irreproducible electrical behaviour. We refer here to long term changes in conductivity under ordinary d.c. test conditions i.e. current flows of the order of a few mA through potential differences of the order of a few volts resulting in mean sample temperatures well below the matrix softening temperature. Two possible reasons for unstable electrical behaviour spring to mind.

(i) Even with low spatially averaged temperatures, substantial local variations in temperature (hot and cold spots) appear to be able to take place in fibre

0022–2461/89 $03.00 + .12

loaded composites [5] due to local variations in fibre distribution and orientation. At hot spots, local changes in polymers microstructure may take place by annealing processes, and fibre–fibre gaps may change due to differential thermal expansion of the fibres and the matrix.

(ii) Local dielectric breakdown through intense electric fields between sharp fibre tips in close proximity.

One purpose of making measurements of the d.c. conductivity σ, of a composite is that its shielding performance at radio and microwave frequencies can readily be evaluated to a fair accuracy, by substitution of σ into the skin depth formula. Instabilities in σ due to mechanisms (i) and (ii) do not necessarily imply that a composite is unsuitable for shielding purposes since the mean induced current levels under normal conditions are likely to be extremely low, particularly when pulsed electromagnetic fields are involved. However, our arguments suggest that bulk composites having fairly substantial conductivity levels greater than $10^{-2}\Omega^{-1}\,cm^{-1}$ would be best tested at the lowest possible levels of applied voltage, a practice which does not appear to be common. The measurements described here use a programmable voltage source which is controllable in intervals of 1 μV down to a level of 50 μV.

A second purpose behind our low level measurements is more academic, namely to answer the question as to whether or not conductive composites are ohmic conductors. To test for this property, the current flow must be varied at constant sample temperature. However, even if a constant temperature enclosure were employed, true equilibrium conditions in the sample could never be achieved as long as local hot spots exist, which is the normal occurrence at power levels of the order of 1 μW or more.

For the above reasons the low voltage characteristics of three composites with different volume fractions of stainless steel fibres in a polypropylene matrix, have been studied.

2. Sample preparation

Raw polypropylene material was obtained from ICI, (Propathene, product code GWM22). Stainless steel fibres were obtained from Bekaert (Beki-shield product code 1/4B/e9/6). This material was supplied in the form of sized, chopped grains of 316L stainless steel alloy drawn fibres. There were approximately 15000 fibres per grain with a nominal fibre length of 6 mm and a diameter of 6.5 μm, whilst the combined diameter of metal with size coating was about 9 μm. Volume fractions were calculated from the equation

$$\text{Vol. fraction} = \{W_{frac}(\tau_m/\tau_f)\}/[1 - W_{frac}(1 - \tau_m/\tau_f)]$$

$$W_{frac} = (\text{mass of fibre})/(\text{mass of matrix} + \text{mass of fibre})$$

where τ_m and τ_f are density of matrix and fibre respectively, using the values $\tau_m = 0.9\,g\,cm^{-3}$ and $\tau_f = 8\,g\,cm^{-3}$. Weights of raw polypropylene and Beki-shield were selected to yield metal volume fractions of 1, 2 and 3% (Table I). No allowance for the weight of the size coating was made in these calculations but the resulting error in the calculated volume fractions is small for present purposes.

TABLE I

Volume fraction (%)	Polypropylene (g)	Beki-shield (g)
1	917	83
2	840	160
3	775	225

To fabricate the plaques two stages were used. First, a single screw extruder (Betol model 2520 EX) was employed. The temperatures of the three extrusion zones were set at 150, 175 and 200° C. The fish-tail die was set at a temperature of 200° C and the screw speed was 90 r.p.m. The output of this stage was in a ribbon form of a mixture of polypropylene and fibres. Then the ribbon was shredded and tumbled in order to get a reasonably homogeneous mixture. In the second stage the shredded mixture was fabricated into plaques. The mixtures were injection moulded on an injection moulder (Sandretto type 6 CV/50 microprocessor controlled with a double film-gated mould cavity). The following processing conditions were employed; screw speed 80 r.p.m., injection speed 36 $cm^3\,sec^{-1}$, injection pressures 82.5 MPa (first phase), 148.5 MPa (second phase), back pressure 0.2 MPa, injection time 1.55 sec and mould temperature 40° C. The barrel temperatures were 180, 200, 240° C in zones 1, 2 and 3 respectively. The plaques obtained were 80 × 80 and 3 mm^3.

3. Electrical measurements

Two edges of the plaques parallel to the injection direction were coated with silver dag to serve as electrodes. These edges were previously milled to ensure the presence of surface-breaking fibres round the edges. It is important to note that this procedure must be adopted in order to measure the values of d.c. conductivity that would be appropriate for substitution in the skin depth formula for estimating microwave shielding performance. This process reduced the sample sides to a uniform length of 79 mm. A specimen supported in a perspex holder is illustrated in Fig. 1. The electric circuit used in these measurements is shown in Fig. 2. The potential drop across the sample electrodes was controlled by means of a programmable voltage source (Keithley Instruments, model 230) whose supply could be varied in 1 μV steps between

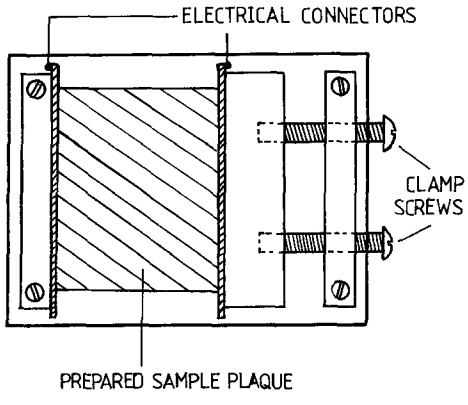

Figure 1 Sample holder.

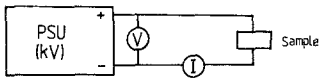

Figure 2 Circuit diagram.

50 μV and 1 V, the internal resistance being maintained at 1 mΩ. The current through the sample was measured to a precision of $\pm 0.3\%$ by the use of a digital electrometer (Keithley Instruments, model 614, measurement range 2 mA to 10^{-15} A). The measured voltage–current characteristics are displayed in Figs 3a to 3c.

4. Sample characterization

4.1. Fibre shapes and distribution

Optical microscope photographs were taken of various plane sections through the plaques both parallel to the flat faces and parallel to the thickness direction and both perpendicular to and normal to the electrodes. Representative examples are shown in Fig. 4. Since the depth of focus was $\pm 50\,\mu$m these photographs show, for a given fibre, the proportion of the fibre which lies within $\pm 50\,\mu$m of a given sample plane.

4.2. Fibre length measurements

In order to investigate the extent of fibre length reduction during processing, initially a burn-off technique was adopted, but it failed by causing extensive damage to the fibre. Therefore, a chemical method of digesting the matrix was used. Small sections of the trial batches were placed in a long-necked reaction flask and 5 ml sulphuric acid added. The flask and contents were then placed in an electrical heating jacket and heated until the acid was fuming. 20–25 ml of 50% w/v hydrogen peroxide was then added dropwise to minimize the violence of the reaction and thus turbulence which could damage the fibres. The exotherm of the reaction causes the mixture to boil gently for about 20 min. The polymer was then completley digested.

The mixture was then greatly diluted in a large beaker and the fibres were allowed to settle. The liquid was decanted and the fibres transferred to a filter funnel, stopped into the top of a Buchner funnel. The fibres were given a final washing and transferred from the funnel to an ultrasonic bath containing microscope slides and a weak teepol detergent solution. When the ultrasonic bath was left running for approximately 10 min, all clumps of fibres were broken up. The slides were placed carefully into a drying oven at 40° C for 3 h, after which time cedar oil was applied to the fibres and a glass cover slip placed on top.

This procedure was carried out for each of a number of trial samples. Each slide was viewed under an optical microscope linked to a Vids two-dot image analyser. This was, in turn, linked to an Apple II computer printer, and graphic board. The computer programme used was a software package specially written for contour fibre length measurement. By simply focusing on fibres, using a suitable set magnification, it was possible to trace the lengths of the individual fibres. In order to obtain statistically significant data, a total of 200 fibres were measured. The computer programme was capable of calculating an individual fibre length from a contour trace using the cursor, recording the information and then giving a mean and a standard deviation value for all 200 fibres measured. A typical frequency distribution histogram for the fibre lengths is shown in Table II.

TABLE II Frequency distribution histogram of sample A

Length (μm)	Count	Count (%)
50–150	6	3.01
150–300	25	12.56
300–450	49	24.62
450–600	50	25.12
600–750	27	13.56
750–900	27	13.56
900–1050	8	4.02
1050–1300	5	2.51
1300–1450	2	1.00
1450–	1	–

5. Discussion of results

5.1. Ohmic behaviour

Each sample was investigated over approximately the

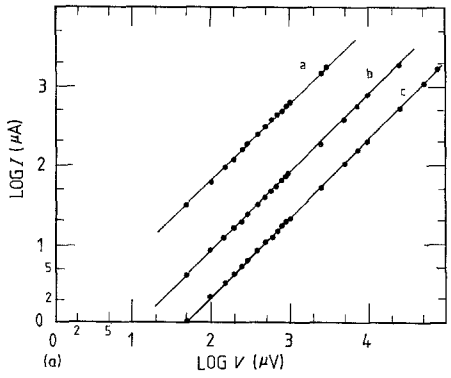

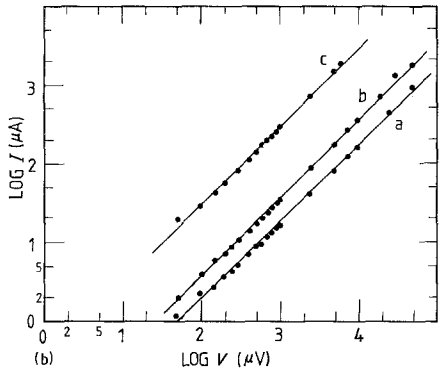

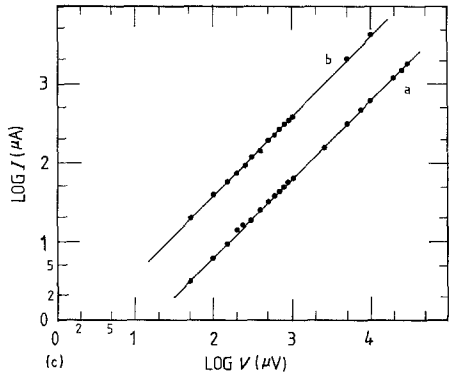

Figure 3 (a) to (c) Voltage–current characteristics for eight different plaques. (a) (a 3%, b 1%, c 2%), (b) (a 1%, b 2%, c 3%), (c) (a 1%, b 3%). Percentages refer to the fibre volume fraction.

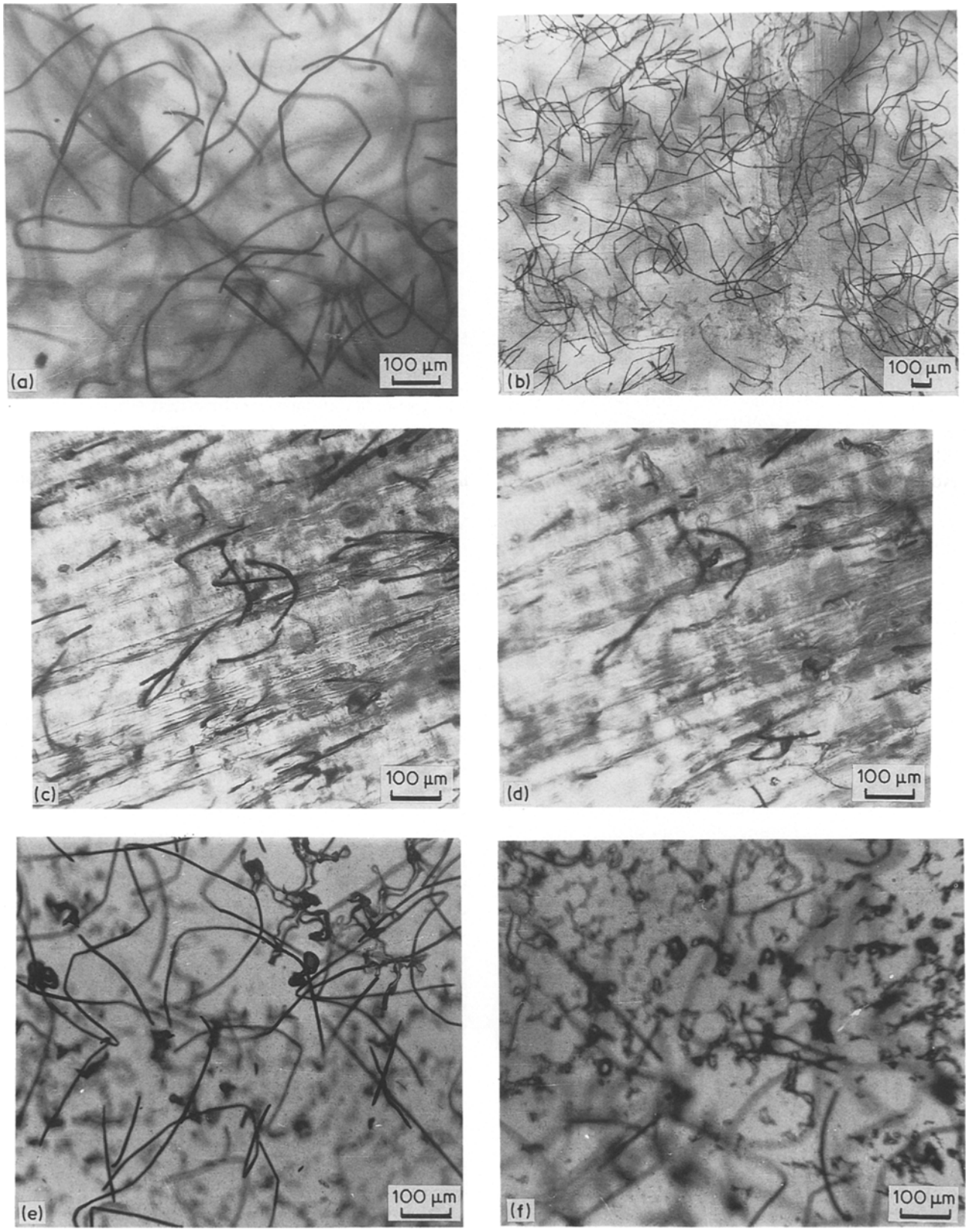

Figure 4 (a) Typical fibre distribution in a sample cut from a plaque and melted between microscopic slides (1% volume fraction). (b) As (a) but 2% volume fraction. (c) Fibre distribution in a sample cut from a plaque. The plane of the photograph is parallel to the faces of the plaque. The horizontal direction in the photograph is parallel to one side of the plaque and the direction of injection moulding (1% volume fraction). (d) As (c) but with the plane of view 50 μm deeper. (e) As (c) but view perpendicularly to the direction of injection moulding. (f) As (e) but with the plane of view 65 μm deeper.

same range of voltage. It is noteworthy that ohmic behaviour is observed in all cases over the four decades of applied voltage from 50 μV to 10 mV (Figs 3a to 3c) and the sample resistivities are given in Table III. Several conclusions stem from this result, by way of the following arguments.

The maximum macroscopic field strength in the samples assuming uniform conditions is $\approx 10^{-3}\,\mathrm{V\,cm^{-1}}$, corresponding to an applied potential difference of 10 mV. The maximum local field can be estimated by considering the extreme case of field lines emerging from the cylindrical surface of a straight 6 mm long

fibre and terminating on the 6.5 μm end face of a second fibre situated in proximity to and oriented perpendicularly to the first fibre. The field near the end face is thus greater than the field round the first fibre by a factor $[6 \times \pi \times 3.25 \times 10^{-3}]/[\pi \times (3.25 \times 10^{-3})^2] \approx 1800$. Surface roughness on the fibres, typically of ≈ 1 μm might cause a further enhancement by a factor $1800 \times (3.25/1)^2 \approx 2 \times 10^4$. Assuming that the second fibre is also 6 mm long and that the fibre gap is relatively small the voltage drop in the macroscopic field, across the two fibre combination, is $10^{-2} \times 6/80 \approx 7.5 \times 10^{-4}$ V. However, locally this voltage drop occurs entirely across the fibre gap because of the low resistivity of the fibres themselves. So for example, for a 10 nm gap the field in the immediate vicinity of the first fibre is $7.5 \times 10^{-4}/10^{-6} = 7.5 \times 10^2$ V cm^{-1}. The field round the tip of the second fibre is then between ≈ 130 V cm^{-1} and 1.6×10^3 V cm^{-1} according to which of the above enhancement factors apply. Now if two fibres are in close proximity i.e. 10 nm apart or less, a significant level of fibre–fibre conductivity may arise by means of quantum mechanical tunnelling through the potential barrier between the fibre, the barrier height being equal to the work function of the fibre material. One of the most comprehensive theoretical studies of tunnelling across metal electrodes was made by Simmons [9, 10] who assumed the presence of a perfect insulator in the gap. Fig. 6 of reference [9, 10] makes clear that non-ohmic tunnelling conductivity will only occur at field strengths $\geqslant 10^5$ V cm^{-1}. Field emission in which charge tunnels through the barrier between a single electrode and the insulator will not occur under the conditions of our experiment since it would require the voltage drop across neighbouring fibres to exceed the sum of the work function and Fermi energy of the fibres.

The more recent theory of tunnelling conductivity by Sheng [11–14] and others [15] in which the effect of thermal noise voltages on the tunnelling probability is taken into account does not alter this conclusion. From our preceding estimates of the maximum local fields prevailing in our experiments we conclude that non-ohmic tunnelling conductivity through insulating material could not occur under the conditions of our experiments, in agreement with the observations. If intrinsic semiconductor material with relatively small energy gaps were present in the gaps between fibres, non-ohmic behaviour can occur at much lower field strengths say 500 V cm^{-1}. Therefore we can add further that the strictly ohmic conditions observed provide no evidence of low energy gap impurities in the polymer matrix contributing significantly to the observed conductivity levels.

TABLE III Resistivity values at different volume fraction

Sample (%)	R (Ω)	ϱ (Ω cm)
1	41	12.00
2	27	8.90
3	3	0.91
1	12	3.64
2	44	13.30
3	2	0.61
1	16	4.85
3	2	0.61

5.2. A percolation model of sample conductivity based on the fibre geometry

Substantial previous work has been carried out on the prediction of the conductivity, σ, arising from the probability of direct contact between metal particles in an insulating matrix [16–18] and Ueda and Tay [18] used a Monte Carlo model to work out the probabilities of formation of fibre chains in carbon composites. However, straight fibres were assumed, a somewhat unrealistic assumption in the case of the steel fibres under consideration by us. Comparison of Fig. 4 and Table II shows that typically the length of fibre visible in a ± 50 μm depth of sample is much less than the mean fibre length. We conclude that the majority of the fibres in the plaques follow curved or kinked paths in three dimensions with radii of curvature typically much smaller than the fibre length. This suggestion can be confirmed by more detailed microscopic examination. Most of the fibres visible in Fig. 4 have blurred rather than sharp edges implying that we are not seeing the true ends of the fibres and that the latter fold away beyond the depth of focus. By varying the depth of focus within the somewhat limited visible range these blurred ends were usually found to become sharper and grow to expose fresh kinked sections.

There can be little doubt that the shapes into which the fibres are distorted have a strong influence on the probability of fibre–fibre contact (at constant volume fraction of fibre), and therefore on the resistivity of the composite. It will be interesting to estimate the number of contacts by making simplifying but realistic assumptions about the fibre contours. For example (Fig. 5), let us assume the fibres to be coiled up into identical helices with a pitch p of the order of or less than the helix diameter D, and let these helices be stacked with axes parallel to each other with a mean axial separation equal to the helix diameter. We assume further that the axes run in the direction of the thickness of the plaques and along any one axis more than one helix may be stacked end-on, the number depending upon the fibre lengths. Under these conditions the probability of contact between fibres with adjacent axes is very high and to a first approximation one may assume one contact per turn.

If the axes of adjacent helices are separated by as little as 10–100 nm or less, conductivity between neighbouring helices takes place by quantum tunnelling or thermal activation across potential barrier of height equal to the work function of the fibres or by other related phenomena depending on the polymer microstructure (including impurities). Thus the conductivity will drop by orders of magnitude even though the volume fraction of fibre has changed by less than $(0.1/D)^{2/3}$ % (D measured in μm). On the other hand if the volume fraction is greater than the amount prescribed by Equation 2, interlocking helices will form and the number of contacts will increase steadily with increasing volume fraction. Thus our idea of parallel helices with axis separations approximately equal to the helix diameter is a possible model

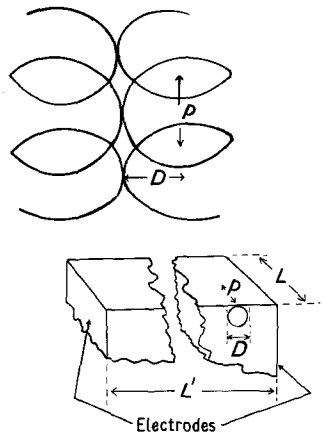

Figure 5 Spiral contact model as discussed in the text.

of the onset of percolation conditions i.e. rapid increase in sample conductivity through the formation of continuous metallic networks between the electrodes. On our model the volume fraction of metal which determines the "percolation threshold" will be

$$V_{pt} = \pi r^2 S/D^2 L \quad (1)$$

where L is the plaque thickness, r the fibre radius, and S the total length of the helix or helices along one axis. Since the length of one helix is given by $n[(\pi D)^2 + p^2]^{1/2}$ where n is the number of turns, then writing $n = L/p$ we obtain

$$V_{pt} = \pi r^2 (D^2 p)^{-1}[(\pi D)^2 + p^2]^{1/2} \quad (2)$$

Taking $p \approx D$ as a special case

$$V_{pt} \approx \pi(\pi^2 + 1)^{1/2}[r/D]^2 \quad (3)$$

In our samples the sharp change in the volume fraction dependence of conductivity was found experimentally to occur at about 1% volume fraction [7]. Substitution of this value for V_{pt} in Equation 3, and taking $r = 3.25\,\mu m$ yields $D \approx 105\,\mu m$. In order of magnitude this value is consistent with Fig. 4, although the visible range of diameter of kinks shows considerable variation.

According to our model the sample can be divided up into rectangular parallelipipeds of volume $D \times D \times p$, and at the percolation threshold there is one fibre–fibre contact between helices with adjacent axes, within each such volume. The mean length of metal between successive contacts will be one half the length of one turn of a helix i.e. $(\frac{1}{2})[(\pi D)^2 + p^2]^{1/2}$. So the resistance of this half turn of metal fibre is

$$R = \tfrac{1}{2}[(\pi D)^2 + p^2]^{1/2}\varrho_f(\pi r^2)^{-1} \quad (4)$$

where ϱ_f is the fibre resistivity.

Defining an effective resistivity ϱ for the plaque, by the relation

$$R = \varrho D[pD]^{-1} = \varrho/p, \quad (5)$$

and combining Equations 4 and 5, we obtain

$$\varrho = \tfrac{1}{2}p[(\pi D)^2 + p^2]^{1/2}(\pi r^2)^{-1}\varrho_f \quad (6)$$

for the special case $D \approx p$ as discussed earlier, this simplifies to

$$\varrho = \tfrac{1}{2}\pi(\pi^2 + 1)^{1/2}(D/r)^2\varrho_f \quad (7)$$

or combining with Equation 3

$$\varrho = (\pi^2 + 1)(2V_{pt})^{-1}\varrho_f \quad (8)$$

This should be regarded as a lower limit for the resistivity when the volume fraction of metal, V, is in vicinity of V_{pt}. Only a very slight decrease in V below V_{pt} will be required for the number of contacts between helices to fall rapidly from the value of one per turn. As V is increased gradually to a value of about V_{pt} the first sharp drop in resistivity will occur when one continuous chain of contacting helices runs from one electrode to the other. If L' is the length of a side of the plaque, the number of such chains when there is one contact per turn, is LL'/Dp. Thus the resistivity of the plaque when only one of these chains is complete is obtained by multiplying the resistivity given by Equation 6 by the factor LL'/Dp, or for the case of $D = p$, the resistivity given by Equations 7 or 8 is multiplied by the factor LL'/D^2. Thus we arrived at the following limits

$$\underset{\text{(All chains complete)}}{(1/2\pi)(\pi^2 + 1)^{1/2}(D/r)^2\varrho_f} \leqslant \varrho \leqslant \underset{\text{(One chain complete)}}{(1/2\pi)(\pi^2 + 1)^{1/2}(r)^{-2}LL'\varrho_f}, \quad \text{for } V \approx V_{pt} \quad (9)$$

or alternatively expressed

$$\tfrac{1}{2}(\pi^2 + 1)(V_{pt})^{-1}\varrho_f \leqslant \varrho \leqslant \tfrac{1}{2}(\pi^2 + 1)(V_{pt})^{-1}(LL'/D^2)\varrho_f \quad (10)$$

substituting $\varrho_f = 74 \times 10^{-6}\,\Omega cm$, $V_{pt} = 0.01$, $L = 3\,mm$, $L' = 80\,mm$ and $r = 3.25\,\mu m$ in the above relations, we obtain

$$4 \times 10^{-2} \leqslant \varrho \leqslant 900\,\Omega cm$$

for the probable range of resistivity values for V in the vicinity of 1%. The observed values of resistivity for $V \approx 1\%$ (Table III and [7]) are 3.6–12 Ω cm i.e. in the middle of the predicted range, on a logarithmic scale. The observed range corresponds to the number of through chains being 0.4 to 1.3% of the maximum number of chains to be expected (i.e. $LL'/D^2 = 2.2 \times 10^4$). Apart from the rapid fall in the number of contacts between helices when V drops below V_{pt}, there are other reasons why the maximum number of electrical contacts predicted by our model cannot be achieved. Firstly consider the typical frequency distribution of fibre lengths shown in Table II. About 80% of fibres have lengths exceeding 450 μm, of sufficient length to be folded into the idealized helices of our model ($D \approx p$) with more than 1.3 turns, whilst 33% could be folded into two turns or more. Secondly and much more important is the size coating on the original bundles of fibres. The size coating has a mean thickness of at least 1 μm. However, our conductivity data suggest that the coating cannot remain completely intact because according to the tunnelling data of Simmons (Fig. 6, [9, 10]), the resistance of a 1 μm thick potential barrier is almost as high as that of a bulk insulator. Therefore we suggest that a proportion of the size coating is totally destroyed during processing, to allow a small fraction (0.4–1.3%) of the maximum number of metal-metal contacts that are possible (on our model) for $V \approx V_{pt}$.

6. Conclusions

A substantial fraction of the fibres in the samples considered have become coiled up three dimensionally into an approximately helical form, thus increasing the probability of fibre–fibre contact. To a first approximation the percolation threshold can be understood in terms of a critical volume fraction at which adjacent helices will start to make contact. A number of relationships can thus be deduced as follows.

(i) The critical volume fraction V_{pt} is proportional to $(r/D)^2$.

(ii) Contrariwise the minimum resistivity at $V \approx V_{pt}$ is proportional to $(D/r)^2$.

(iii) The maximum resistivity at $V \approx V_{pt}$ is proportional to $(1/r)^2$.

(iv) The number of helical fibres N available to form mutual contacts will increase with mean fibre length F. Thus the resistivity for $V \approx V_{pt}$ tends to decrease with increasing F. Thus it pays to adjust processing conditions for minimum fibre breakage providing this does not conflict with the conditions required to achieve good fibre dispersion.

(v) For a given F and processing conditions, the forces generated during processing will bend the fibres more readily as the mean fibre aspect ratio ($F/r = A$) increases. If A is very small, fibres that were initially straight will not bend significantly so that no helices are formed, N will tend to zero and V_{pt} will become very large. On the other hand when A becomes very large D will become small or N may become small due to fibre breakage, and in either case V_{pt} will again become large. Consequently there exists an intermediate (optimum) value of A for which V_{pt} is a minimum.

For most practical applications the resistivity levels of interest would require $V \leqslant V_{pt}$. Certainly if reproducibility of resistivity in repetitive manufacture of samples is required the range $V < V_{pt}$ is precluded because of the rapid variation of ϱ with V. For cost effectiveness it might often be considered desirable to minimize the metal content required to achieve a prescribed value of resistivity. In view of the contrasting dependence of ϱ (for $V \approx V_{pt}$) and V_{pt} on fibre properties, as summarized in (i) and (ii) above, this minimum metal volume fraction does not necessarily coincide with V_{pt}. However, by the same token the smaller is V_{pt} the greater is the range of resistivities that can be achieved in a controlled manner by varying V from V_{pt} upwards. From this viewpoint it will often be desirable to minimize V_{pt}. In this respect experiments to determine the fibre radius, fibre aspect ratio, and processing conditions which maximize D/r seem well worthwhile.

Acknowledgement

The authors would like to thank the SERC for their financial support for this work under the Specially Promoted Programme on electroactive polymers, and Dr. Adriaensen of Bekaert Ltd for helpful discussion and the supply of fibres.

References

1. D. M. BIGG, *Polym. Eng. Sci.* **17** (1977) 842.
2. D. M. BIGG and D. E. STUTZ, *Polym. Comp.* **4** (1983) 40.
3. V. E. GUL and N. S. MAIZEL, *Plastic Msaay* **5** (1965) 49.
4. J. GURLAND, *Trans. Met. Soc. AIME* **236** (1966) 642.
5. B. BRIDGE, M. J. FOLKES, H. JAHANKHANI, *J. Mater. Sci.* **23** (1988) 1948-54.
6. *Idem, ibid.* **23** (1988) 1955-60.
7. S. FERIDOONIAN, MPhil thesis, Brunel University (1986).
8. D. ADRIAENSEN, Private communication.
9. J. G. SIMMONS, *J. Appl. Phys.* **34** (1963) 1793.
10. *Idem, ibid.* **35** (1964) 2472.
11. P. SHENG, *Phys. Rev. B* **21** (1980) 2180.
12. P. SHENG, E. K. SICHEL and J. L. GITTLEMAN, *Phys. Rev. Lett.* **40** (1973) 1197.
13. E. K. SICHEL, J. L. GITTLEMAN and P. SHENG, *Phys. Rev. B* **18** (1978) 5712.
14. C. M. SOUKOULIS, J. V. JOSE, E. N. ELONOMOU and P. SHENG, *Phys. Rev. Lett.* **50** (1983) 5712.
15. R. D. SHERMAN, L. M. MIDDLEMAN and S. M. JACOBS, *Polym. Eng. Sci.* **23** (1983) 36.
16. R. L. McCULLOUGH, *Comp. Tech.* **22** (1985) 3.
17. A. MALLIARIS and D. T. TURNER, *J. Appl. Phys.* **42** (1971) 614.
18. N. UEDA and M. TAYS, Proceedings 5th Conference in Composite Materials ICCM-V, San Diego, California, Aug. 1985 (Metallurgical Society, Warrendale, Pa.) p. 1727.

Received 1 March
and accepted 1 June 1988